REPORT DOCUMENTATION PAGE

Form Approved OMB NO. 0704-0188

1. REPORT DATE (DD-MM-YYYY)	2. REPORT TYPE	3. DATES COVERED (From - To)
10-07-2015	Final Report	10-Sep-2012 - 9-Apr-2015

4. TITLE AND SUBTITLE

Final Report: Supramolecular Polymers With Multiple Types of Binding Motifs: From Fundamental Studies to Multifunctional Materials

5a. CONTRACT NUMBER
W911NF-12-1-0339

5b. GRANT NUMBER

5c. PROGRAM ELEMENT NUMBER
611102

6. AUTHORS

Stuart Rowan, Christoph Weder

5d. PROJECT NUMBER

5e. TASK NUMBER

5f. WORK UNIT NUMBER

7. PERFORMING ORGANIZATION NAMES AND ADDRESSES

Case Western Reserve University
10900 Euclid Ave.

Cleveland, OH 44106 -4919

8. PERFORMING ORGANIZATION REPORT NUMBER

9. SPONSORING/MONITORING AGENCY NAME(S) AND ADDRESS (ES)

U.S. Army Research Office
P.O. Box 12211
Research Triangle Park, NC 27709-2211

10. SPONSOR/MONITOR'S ACRONYM(S)
ARO

11. SPONSOR/MONITOR'S REPORT NUMBER(S)
62050-CH.9

12. DISTRIBUTION AVAILIBILITY STATEMENT

Approved for Public Release; Distribution Unlimited

13. SUPPLEMENTARY NOTES

The views, opinions and/or findings contained in this report are those of the author(s) and should not contrued as an official Department of the Army position, policy or decision, unless so designated by other documentation.

14. ABSTRACT

This research project is focused on the development and investigation of a new class of multi-stimuli-responsive polymers, which are designed exhibit different responses upon exposure to different stimuli. The concept here is the development of materials systems that consist of different stimuli-responsive components which can be designed to work orthogonally or interact with each other such a way that exposure to more than one stimulus alters the state of the system in a nonlinear manner. This report focuses on the development a range on new material that includes studies metallo and hydrogen bonded supramolecular polymers that exhibit defect healing characteristics and multi

15. SUBJECT TERMS

Active Polymers, Supramolecular, Metal coordination, stimuli-responsive. liquid crystal elastomers

16. SECURITY CLASSIFICATION OF:			17. LIMITATION OF ABSTRACT	15. NUMBER OF PAGES	19a. NAME OF RESPONSIBLE PERSON
a. REPORT	b. ABSTRACT	c. THIS PAGE			Stuart Rowan
UU	UU	UU	UU		19b. TELEPHONE NUMBER 216-368-4242

Report Title

Final Report: Supramolecular Polymers With Multiple Types of Binding Motifs: From Fundamental Studies to Multifunctional Materials

ABSTRACT

This research project is focused on the development and investigation of a new class of multi-stimuli-responsive polymers, which are designed exhibit different responses upon exposure to different stimuli. The concept here is the development of materials systems that consist of different stimuli-responsive components which can be designed to work orthogonally or interact with each other such a way that exposure to more than one stimulus alters the state of the system in a nonlinear manner. This report focuses on the development a range on new material that includes studies metallo and hydrogen bonded supramolecular polymers that exhibit defect healing characteristics and multi-responsive actuators. It also report on a new class of supramolecular glasses.

Enter List of papers submitted or published that acknowledge ARO support from the start of the project to the date of this printing. List the papers, including journal references, in the following categories:

(a) Papers published in peer-reviewed journals (N/A for none)

Received		Paper
07/01/2015	5.00	Brian T. Michal, Blayne M. McKenzie, Simcha E. Felder, Stuart J. Rowan. Metallo-, Thermo-, and Photoresponsive Shape Memory and Actuating Liquid Crystalline Elastomers, Macromolecules, (05 2015): 3239. doi: 10.1021/acs.macromol.5b00646
07/06/2015	6.00	Souleymane Coulibaly, Christian Heinzmann, Frederick L. Beyer, Sandor Balog, Christoph Weder, Gina L. Fiore. Supramolecular Polymers with Orthogonal Functionality, Macromolecules, (12 2014): 8487. doi: 10.1021/ma501492u
07/06/2015	7.00	Yoan C. Simon, Gina L. Fiore, Christoph Weder. Mechanically Triggered Responses of Metallosupramolecular Polymers, CHIMIA International Journal for Chemistry, (09 2014): 666. doi: 10.2533/chimia.2014.666
08/24/2014	3.00	Diederik W. R. Balkenende, Souleymane Coulibaly, Sandor Balog, Yoan C. Simon, Gina L. Fiore, Christoph Weder. Mechanochemistry with Metallosupramolecular Polymers, Journal of the American Chemical Society, (07 2014): 10493. doi: 10.1021/ja5051633
08/24/2014	2.00	Souleymane Coulibaly, Anita Roulin, Sandor Balog, Mahesh V. Biyani, E. Johan Foster, Stuart J. Rowan, Gina L. Fiore, Christoph Weder. Reinforcement of Optically Healable Supramolecular Polymers with Cellulose Nanocrystals, Macromolecules, (01 2014): 152. doi: 10.1021/ma402143c
08/24/2014	4.00	Christian Heinzmann, Souleymane Coulibaly, Anita Roulin, Gina L. Fiore, Christoph Weder. Light-Induced Bonding and Debonding with Supramolecular Adhesives, ACS Applied Materials & Interfaces, (04 2014): 4713. doi: 10.1021/am405302z
08/26/2013	1.00	Colin A. Jaye, Emily J. Spencer, Stuart J. Rowan, Brian T. Michal. Inherently Photohealable and Thermal Shape-Memory Polydisulfide Networks, ACS Macro Letters, (08 2013): 694. doi: 10.1021/mz400318m
TOTAL:	**7**	

Number of Papers published in peer-reviewed journals:

(b) Papers published in non-peer-reviewed journals (N/A for none)

Received	Paper

TOTAL:

Number of Papers published in non peer-reviewed journals:

(c) Presentations

Stuart Rowan: 1 Aug 2014 - 9 April 2015
April 2015 Université de Montréal, Montreal, Canada
Invited Lecture: Using Dynamic Chemistry as a Route to New Stimuli-responsive Materials
April 2015 McGill University, Montreal, Canada
Invited Lecture: Using Dynamic Chemistry as a Route to New Stimuli-responsive Materials
Mar 2015 Miami University, Ohio
Invited Lecture: Using Dynamic Chemistry as a Route to New Stimuli-responsive Materials
Feb 2015 University of Chicago, Institute for Molecular Engineering,
Invited Lecture: Using Dynamic Chemistry as a Route to New Stimuli-responsive Materials
Feb 2015 Case Western Reserve University, Department of Chemical Engineering
Invited Lecture: Using Dynamic Chemistry as a Route to New Stimuli-responsive Materials
Feb 2015 University of Miami, Department of Chemistry
Invited Lecture: Using Dynamic Chemistry as a Route to New Stimuli-responsive Materials
Jan 2015Macromolecular Materials GRC
Invited Lecture: Using Dynamic Chemistry as a Route to New Stimuli-responsive Materials
Dec 2014 Zing Polymer Conference
Invited Lecture: Using Dynamic Chemistry as a Route to New Stimuli-responsive Materials
Nov 2014 Departments of Bioengineering/Material Sci. UC Berkeley
Invited Lecture: Using Dynamic Chemistry as a Route to New Stimuli-responsive Materials and Bioimplants
Sep 2014 UNC Chapel Hill MRS Student Seminar
Invited Lecture: Using Dynamic Chemistry to Access Stimuli-Responsive Materials
Aug. 2014 ACS San Francisco ACS-PMSE/CCS-PD Joint Symposium
Invited Lecture: Using Dynamic Chemistry to Access Stimuli-Responsive Materials

C. Weder
"Stimuli-Responsive Hydrogen-Bonded Supramolecular Polymers"
Plenary Lecture, International Symposium on Stimuli-Responsive Materials, October 27, 2014; Santa Rosa, CA

2nd Biomimicry Europe Innovation and Finance Summit"
September 4, 2014; Zürich, Switzerland

"Mechanically (And Other) Responsive Polymers"
ERC Grantees Conference, August 28, 2014; Berlin, Germany

"Stimuli-Responsive Hydrogen-Bonded Supramolecular Polymers"
ACS Fall Meeting 2014, August 12, 2014; San Francisco, CA, USA

"Stimuli-Responsive Metallosupramolecular Polymers"
ACS Fall Meeting 2014, August 11, 2014; San Francisco, CA, USA

Talks D. Balkenende
"Optically responsive supramolecular glasses"
Swiss Soft Days, 02.10.14, Lausanne, Switzerland

"Optically responsive supramolecular glasses"
ACS Spring Meeting 2015, March 25, 2015; Denver, CO, USA

Number of Presentations: 18.00

Non Peer-Reviewed Conference Proceeding publications (other than abstracts):

Received	Paper

TOTAL:

Number of Non Peer-Reviewed Conference Proceeding publications (other than abstracts):

Peer-Reviewed Conference Proceeding publications (other than abstracts):

Received	Paper

TOTAL:

Number of Peer-Reviewed Conference Proceeding publications (other than abstracts):

(d) Manuscripts

Received	Paper	
07/06/2015	8.00	Diederik W. R. Balkenende, Christophe A. Monnier, Gina L. Fiore, Christoph Weder. Optically responsive supramolecular polymer glasses, Nature Chemistry (submitted) (05 2015)

TOTAL: **1**

Number of Manuscripts:

Books

Received Book

TOTAL:

Received Book Chapter

TOTAL:

Patents Submitted

Stimulus-Responsive Supramolecular Glasses

Patents Awarded

Awards

Stuart J Rowan:
CWRU Faculty Distinguished Research Award
ACS POLY Fellow
Herman Mark Scholar Award (ACS POLY)

D. Balkenende:
2015 Chemistry Travel Award of the Swiss Academy of Sciences (SCNAT), the Swiss Chemical Society (SCS) and the Swiss Society for Food and Environmental Chemistry (SSFEC). The award was granted for participation at the ACS Spring Meeting 2015 in Denver.

Graduate Students

NAME	PERCENT_SUPPORTED	Discipline
Katie Greenman	0.80	
Adriane Miller	0.20	
Brian Michal	0.00	
Diederik Balkenende	1.00	
FTE Equivalent:	**2.00**	
Total Number:	**4**	

Names of Post Doctorates

NAME	PERCENT_SUPPORTED
Thomas Spilker	0.00
FTE Equivalent:	**0.00**
Total Number:	**1**

Names of Faculty Supported

NAME	PERCENT_SUPPORTED	National Academy Member
Stuart J Rowan	0.00	
Christoph Weder	0.00	
FTE Equivalent:	**0.00**	
Total Number:	**2**	

Names of Under Graduate students supported

NAME	PERCENT_SUPPORTED	Discipline
Jonathan Onorato	0.00	Macromolecular Sci & Eng
Claire Plunkett	0.00	Macromolecular Sci & Eng
FTE Equivalent:	**0.00**	
Total Number:	**2**	

Student Metrics

This section only applies to graduating undergraduates supported by this agreement in this reporting period

The number of undergraduates funded by this agreement who graduated during this period: 1.00

The number of undergraduates funded by this agreement who graduated during this period with a degree in science, mathematics, engineering, or technology fields:..... 1.00

The number of undergraduates funded by your agreement who graduated during this period and will continue to pursue a graduate or Ph.D. degree in science, mathematics, engineering, or technology fields:..... 1.00

Number of graduating undergraduates who achieved a 3.5 GPA to 4.0 (4.0 max scale):..... 1.00

Number of graduating undergraduates funded by a DoD funded Center of Excellence grant for Education, Research and Engineering:..... 0.00

The number of undergraduates funded by your agreement who graduated during this period and intend to work for the Department of Defense 0.00

The number of undergraduates funded by your agreement who graduated during this period and will receive scholarships or fellowships for further studies in science, mathematics, engineering or technology fields: 0.00

Names of Personnel receiving masters degrees

NAME	
Claire Plunkett	
Total Number:	**1**

Names of personnel receiving PHDs

NAME
Total Number:

Names of other research staff

NAME	PERCENT_SUPPORTED
FTE Equivalent:	
Total Number:	

Sub Contractors (DD882)

Inventions (DD882)

Scientific Progress

See attachment

Technology Transfer

There have been strong interactions with Rick Bayer (ARL) who has been involved with the project helping to understand the morphology of the materials through SAXS and TEM studies. He was on one paper already this year and will be on a second paper that is currently being written

Final Report

Supramolecular Polymers With Multiple Types of Binding Motifs: From Fundamental Studies to Multifunctional Materials

Report Period Begin Date: 08/01/2014

Report Period End Date: 04/31/2015

Table of Contents

List of Figures and Tables

Blends of Supramolecular Polymer with Orthogonal Interactions and Responsiveness

In **Year 3**, we completed the systematic investigation of the structure-property relationships and the stimuli-responsive nature of supramolecular polymers with chemically orthogonal binding motifs and multi-responsive, multifunctional behavior. The materials studied were made by blending two supramolecular materials based on poly(ethylene-*co*-butylene) (PEB) telechelics decorated with either 2,6-bis(1′-methylbenzimidazolyl) pyridine (Mebip) ligands that can coordinate to metal ions ([M(BKB)]A_2; M = Fe^{2+}, Zn^{2+}; A = NTf_2^-, ClO_4^-,) or 2-ureido-4[1H]-pyrimidinone (UPy) motifs (UPy-PEB-UPy) that can dimerize in a self-complimentary fashion (**Figure 1**).

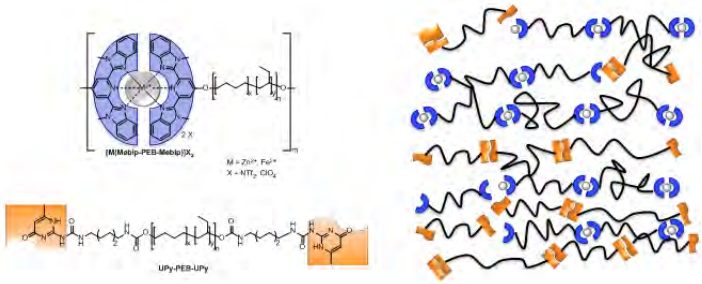

Figure 1. Schematic representation of supramolecular polymer blends with orthogonal functional groups.

In **Year 2**, we had already shown that binding is not orthogonal for Zn(BKB)]$(NTf_2)_2$/(UPy-PEB-UPy) on account of the dynamic nature of both Zn-Mebip and UPy-UPy interactions, and a propensity of Zn^{2+} to also bind to the UPy motif. By contrast, UV-Vis spectroscopic titration experiments revealed that equimolar mixtures of [Fe(BKB)]$(ClO_4)_2$ and (UPy-PEB-UPy) show orthogonal binding. These results served as a basis for the preparation of solid blends of this system, where the [Fe(BKB)]$(ClO_4)_2$/(UPy-PEB-UPy) ratio was systematically varied between 1:1 and 1:0.3. Using dynamic mechanical thermoanalysis (DMTA), we had shown in **Year 2** that blends with a [Fe(BKB)]$(ClO_4)_2$/(UPy-PEB-UPy) ratio of 1:0.7 or 1:0.5 show two distinct transitions associated with the disassembly of hard-phases composed of UPy (ca. 60 °C) and Fe^{2+}-Mebip (ca. 180 °C) motifs, respectively. The Fe^{2+}-Mebip interactions were further selectively disrupted by the addition of a competitive ligand, demonstrating that each supramolecular motif can be targeted with either a thermal or chemical stimulus.

To refine the morphological studies conducted in **Year 2**, in **Year 3** we conducted small-angle X-ray scattering (SAXS) and high-angle annular dark field STEM (HAADF-STEM) experiments in collaboration with Frederick Beyer at ARL. The SAXS spectra of {[Fe(BKB](ClO$_4$)$_2$}$_{1.0}$(UPy-PEB-UPy)$_x$ (x = 1, 0.7, 0.5, 0.3 eq) blends with varying UPy-PEB-UPy content show distinct Bragg diffraction peaks up to the second order, which mirror those of the neat [Fe(BKB)]$(ClO_4)_2$ and suggest that most of these materials adopt lamellar morpholo-

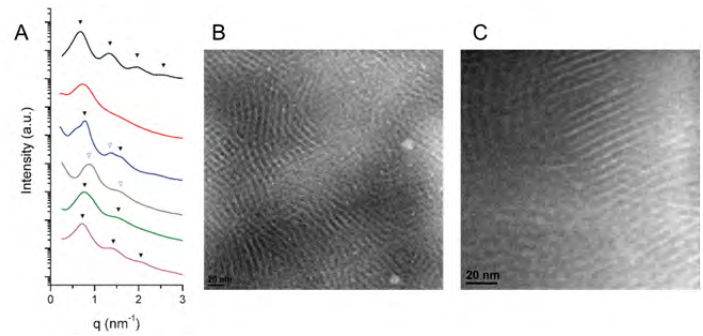

Figure 2. Morphology of supramolecular polymer blends. (a) SAXS spectra of the metallosupramolecular polymer [Fe(BKB)]$(ClO_4)_2$ (—), the neat UPy-PEB-UPy (—), and blends of [Fe(BKB)]$(ClO_4)_2$ and UPy-PEB-UPy with a ratio of 1:1 (—), 1:0.7 (—), 1:0.5 (—) and 1:0.3 (—). The closed and open triangles show scattering maxima corresponding to lamellar and cylindrical morphologies. (b) TEM image of [Fe(BKB)]$(ClO_4)_2$, showing a lamellar morphology. (c) TEM image of {[Fe(Mebip-PEB-Mebip)]$(ClO_4)_2$}$_{1.0}$(UPy-PEB-UPy)$_{0.7}$, showing a mixture of hexagonally-packed cylinders and lamellar structures.

gies with significant long range order (**Figure 2a**). However, the blend of equimolar {[Fe(Mebip-PEB-Mebip)]$(ClO_4)_2$}$_{1.0}$(UPy-PEB-UPy)$_{1.0}$ shows a complex scattering pattern. Fitting of the data suggests that this is likely due to the presence of both lamellar and cylinder morphologies, whereas the {[Fe(Mebip-PEB-Mebip)]$(ClO_4)_2$}$_{1.0}$(UPy-PEB-UPy)$_{0.7}$ blend adopts a cylindrical morphology (**Figure 2a**). TEM images of the [Fe(Mebip-PEB-Mebip)]$(ClO_4)_2$ homopolymer control and {[Fe(Mebip-PEB-Mebip)]$(ClO_4)_2$}$_{1.0}$(UPy-PEB-UPy)$_{0.7}$ confirm the presence of lamellar and hexagonally-packed cylinders morphologies, respectively (**Figure 2b,c**). The equimolar {[Fe(Mebip-PEB-Mebip)]$(ClO_4)_2$}$_{1.0}$(UPy-PEB-UPy)$_{1.0}$ blend also presents scattering features corresponding to the neat UPy-PEB-UPy (densely packed fibers), suggesting that both a long range lamellar morphology and short range packed fibers are present.

In summary, we demonstrated that [Fe(Mebip-PEB-Mebip)]$(ClO_4)_2$/(UPy-PEB-UPy) blends show both, orthogonal supramolecular binding *and* orthogonal stimuli responsiveness, which results in orthogonal materials responses. While a few supramolecular polymer systems with orthogonal binding (in solution) have been demonstrated in the past, we believe that selective switching of properties has been achieved for the first time. The basic concept can be adapted to a broad range of supramolecular polymers based on other binding motifs. The results of this study have been published in *Macromolecules*.[1]

The Effect of Macromonomer and Counterion in Metallo-Supramolecular Polymers

The success of the above Fe(II)-based system lead us to examine the structure property relationships of the Fe(II)-containing metallo-supramolecular polymers. Specifically given the larger binding constant of the Fe(II):$MeBip_2$ complex (logβ ca. 10^{10} M^{-2}) vs Zn(II):$MeBip_2$ complex (logβ ca. 10^6 M^{-2}), which allows the selectivity above, we were interesting in using this as a platform to better understand the effect of counterion on this class of materials. In prior ARO funded work (and in collaboration with Beyer (ARL)) we had shown the effect of adding in a metal ion that forms weaker MeBip complexes than Zn(II) and shown that if the poly(ethylene-*co*-butylene) core in the MeBip-PEB-MeBip is replaced with a poly(tetrahydrofuran) core (MeBip-PTHF-MeBip) that much weaker phase segregation and corresponding much weaker are obtained.[2] Specifically, we were now interested in how the stronger binding Fe(II):$MeBip_2$ complex would assemble with the more polar BTB and how the counterion could be used to impact/control the properties (i.e. can it be used to tune the morphology).

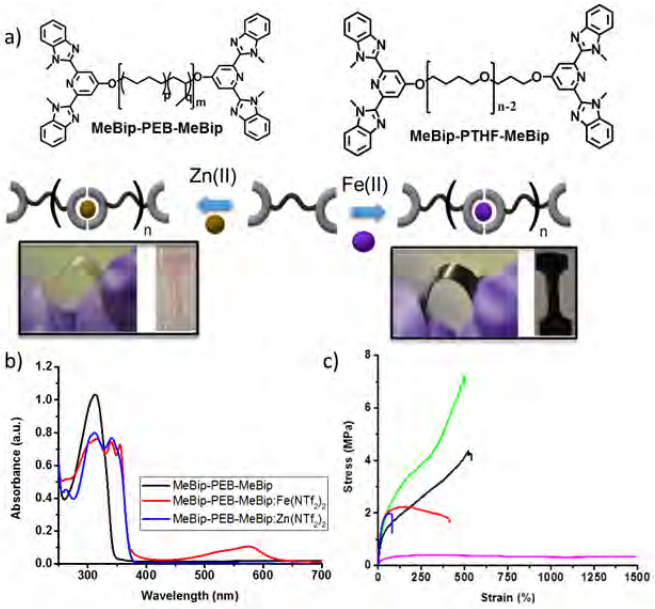

Figure 3. (a) Structures of the two macromonomers in this study and images of the metallo-supramolecular polymers produced by complexing with the transition metal salt. (b) Electronic absorption spectra of the macromonomer (black), iron supramolecular polymer (red), and zinc supramolecular polymer (blue). (c) Tensile results of representative samples of metallopolymers MeBip-PTHF-MeBip:X where X = $Fe(NTf_2)_2$ (pink), $Fe(ClO_4)_2$ (black), $Fe(BF_4)_2$ (green), $Zn(ClO_4)_2$ (blue), $Zn(BF_4)_2$ (red).

We prepared several new metallo-supramolecular polymers of similar molecular weight from 2,6-bis(N-methylbenzimidazolyl) pyridine (BIP) end-capped poly(ethylene-*co*-butylene) (Mebip-PEB-Mebip) or poly(tetrahydrofuran) (Mebip-PTHF-Mebip) by complexing with zinc (II) or iron (II) with several different anions including bistriflimide, tetrafluroborate, and perchlorate, **Figure 3**. The healing in these compounds depends on a photo/thermal conversion process where light is absorbed by the metal-ligand complex and converted to heat by nonradiative decay pathways. The choice of iron (II) modifies the supramolecular polymers in two ways. First, it introduces a metal-to-ligand charge transfer absorption in the visible observed between 450 – 620 nm (**Figure 3**) that allows the photothermal conversion process to happen with visible light irradiation. Secondly, it has a stronger binding constant to the BIP end group of the telechelic macromonomer (10^{10} vs 10^{6}). The higher binding constant results in higher molecular weight supramolecular polymers and slower exchange rates that may result in different mechanical properties. We expect the morphology of these materials to be dependent upon the choice of macromonomer due to the relative polarity of the poly(ethylene-*co*-butylene) and poly(tetrahydrofuran) cores. This will impact the solubility of the metal complexes within this polymer layer, which may allow for deviation from the lamellar morphology seen in the poly(ethylene-*co*-butylene) materials previously investigated (vide supra).

The complexes prepared with MeBip-PTHF-MeBip show a wide array of mechanical properties depending upon the chosen metal and counter anion. The tensile testing results can be seen in Table 1 and representative samples in **Figure 3c**. From these data, we data see there are three regimes the metallopolymers perform in. MeBip-PTHF-MeBip:$Zn(ClO_4)_2$ stretches to a strain of ~70% and previous investigations have shown this material have a lamellar morphology.[2] The three compounds MeBip-PTHF-MeBip:$Zn(BF_4)_2$, Mebip-PTHF-Mebip:$Fe(BF_4)_2$, and MeBip-PTHF-MeBip:$Fe(ClO_4)_2$ show a strain of ~500 % at break. The compound MeBip-PTHF-MeBip:$Fe(NTf_2)_2$ stretches to 1500% before it breaks and its counterpart MeBip-PTHF-MeBip:$Zn(NTf_2)_2$ does not form a robust film but instead forms a tacky, viscous liquid.

Table 1: Mechanical testing data of metallosupramolecular polymers prepared with MeBip-PTHF-MeBip

Sample MeBip-PTHF-MeBip	Young's Modulus (MPa)	Stress at Break (MPa)	Strain at Break (%)	Toughness (mJ/mm^3)
$Zn(NTf_2)_2$	-	-	-	-
$Zn(BF_4)_2$	15.2 ± 1.1	2.39 ± 0.21	459± 120%	10.2 ± 3.7
$Zn(ClO_4)_2$	16.4 ± 5.2	2.01 ± 0.26	69 ± 7%	1.09 ± 0.20
$Fe(BF_4)_2$	7.57 ± 1.20	6.58 ± 0.60	475 ± 41%	17.9 ± 2.6
$Fe(NTf_2)_2$	0.36 ± 0.34	0.31 ± 0.08	1416 ± 184%	2.90 ± 1.95
$Fe(ClO_4)_2$	11.8 ± 2.0	2.12 ± 0.26	474 ± 85%	13.9 ± 2.8

In order to explain the varying mechanical properties seen in the materials prepared with the poly(tetrahydrofuran) macromonomer MeBip-PTHF-MeBip, we undertook a morphological investigation to look at the effect of the metal and anion on the solid state phase separation in collaboration with Frederick Beyer of the Army Research Laboratory. The small angle X-ray scattering spectra show a significant difference in the ordering of the compounds MeBip-PTHF-MeBip:$Zn(NTf_2)_2$, MeBip-PTHF-MeBip:$Fe(NTf_2)_2$, and MeBip-PTHF-MeBip:$Zn(BF_4)_2$, MeBip-PTHF-MeBip:$Fe(BF_4)_2$. MeBip-PTHF-MeBip:$Fe(BF_4)_2$ shows very little long range order with only one scattering peak. However, the Zn analog MeBip-PTHF-MeBip:$Zn(BF_4)_2$

shows a peak at q* and q*√2 suggesting a cylindrical morphology. The two compounds MeBip-PTHF-MeBip:$Zn(NTf_2)_2$ and MeBip-PTHF-MeBip:$Fe(NTf_2)_2$ show multiple scattering peaks at q*, 2q*, and q*, 2q*, 3q*, respectively, indicating a lamellar morphology, but much less ordered than see in compounds prepared with MeBip-PEB-MeBip.[1] The material MeBip-PTHF-MeBip:$Fe(BF_4)_2$ was also studied with HAADF-STEM and the nanoscale morphology was found to not be lamellar, but it was fragmented with the metal hard phase seemingly acting like physical crosslinks within the poly(tetrahydrofuran) phase, **Figure 4a** (light areas corresponding to high Fe content). This difference in morphology may be understood in terms of the greater interaction of the metal complex with the poly(THF) reducing the desire to phase separate. This alternate morphology may also account for the highly elastic nature of this material.

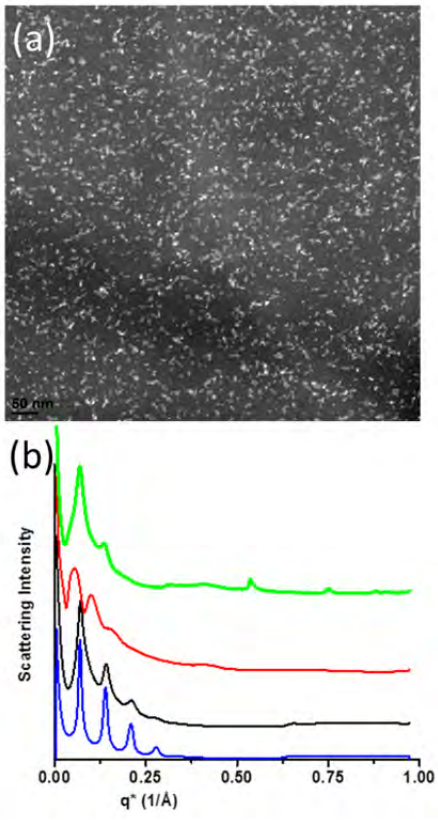

Figure 4. (a) HAADF-STEM micrograph of MeBip-PTHF-MeBip:$Fe(BF_4)_2$. (b) SAXS spectra of MeBip-PEB-MeBip:$Zn(NTf_2)_2$ (blue), MeBip-PEB-MeBip:$Fe(NTf_2)_2$ (black), MeBip-PTHF-MeBip:$Zn(NTf_2)_2$ (red), MeBip-PTHF-MeBip:$Fe(NTf_2)_2$ (green).

As a control, the mechanical properties of the metallo-supramolecular polymers were investigated for materials prepared with poly(ethylene-*co*-butylene) can be nicely seen the comparative series of MeBip-PEB-MeBip:$Zn(NTf_2)_2$, MeBip-PEB-MeBip:$Fe(NTf_2)_2$, MeBip-PTHF-MeBip:$Zn(NTf_2)_2$, MeBip-PTHF-MeBip:$Fe(NTf_2)_2$. There is a dramatic difference in the mechanical properties of films of different macromonomers, MeBip-PEB-MeBip or MeBip-PTHF-MeBip.The effects are immediately noticeable in the $Zn(NTf_2)_2$ materials; the complex with MeBip-PEB-MeBip is a robust film that stretches to 70%, whereas the complex with MeBip-PTHF-MeBip is a highly viscous oil with no mechanical strength. MeBip-PEB-MeBip:$Fe(NTf_2)_2$ is a robust tough film whereas MeBip-PTHF-MeBip:$Fe(NTf_2)_2$ is slightly tacky, and much more elastic with a strain at break 70% vs 1500%, respectively. The materials prepared with MeBip-PEB-MeBip show highly ordered lamellar phase separated morphologies by small angle X-ray scattering, whereas the materials prepared with MeBip-PTHF-MeBip show dramatically reduced long range order, but still an apparent lamellar ordering, **Figure 4b**. The mechanical properties of MeBip-PEB-MeBip:$Zn(BF_4)_2$, MeBip-PEB-MeBip:$Fe(BF_4)_2$ and they show strains of 70% at break similar to MeBip-PEB-MeBip:$Zn(NTf_2)_2$, MeBip-PEB-MeBip:$Fe(NTf_2)_2$, whereas MeBip-PTHF-MeBip:$Zn(BF_4)_2$, MeBip-PTHF-MeBip:$Fe(BF_4)_2$ break at ~500% strain. The SAXS data of MeBip-PTHF-MeBip:$Zn(BF_4)_2$, MeBip-PTHF-MeBip:$Fe(BF_4)_2$ also show very strong scattering at q*, 2q*, 3q*, and 4q* indicating a highly ordered lamellar morphology. This highlights the role of the poly(tetrahydrofuran) macromonomer (MeBip-PTHF-MeBip) in the enhanced sensitivity to the metal and anion.

It is apparent, the mechanical properties of these metallo-supramolecular polymers is highly sensitive to the chosen macromonomer, metal, and counter anion with these materials

showing several different morphologies. Ongoing experiments are currently examining the effect of the molecular weight of the macromonomer on the subsequent morphology of the metallo-supramolecular polymers and also further investigation of the morphology of the current materials by electron microscopy. Light induced healing experiments are also underway and preliminary data indicate the iron materials can be healed with visible light.

Supramolecular Building Blocks with Orthogonal Binding Motifs

In **Year 3** we started to explore the synthesis, assembly, and stimuli-induced disassembly of supra-molecular building blocks that feature both hydrogen-bonding UPy, as well as cyano-substituted oligo(phenylene vinylene) (cyano-OPV) motifs (**Figure 5a**). The latter are well known to exhibit π-π interactions and to change their fluorescence color upon self-assembly, on account of excimer formation.[3] Some of us previously demonstrated that the thermally or mechanically induced (dis)assembly of cyano-OPVs in blends of such dyes and various matrix polymers can be used to create thermochromic and mechanochromic materials. Here, we sought to utilize the cyano-OPV motif to create stimuli-responsive materials based on *one* building block that comprised *multiple* supramolecular binding motifs with orthogonal binding characteristics.

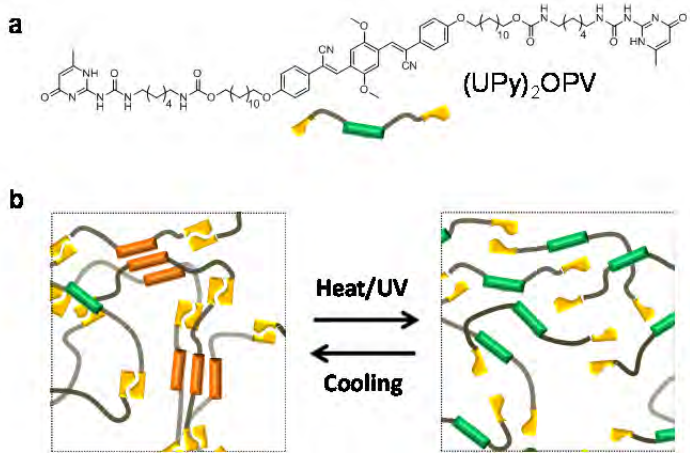

Figure 5. Supramolecular building blocks with orthogonal binding motifs. (a) Molecular structure of $(UPy)_2OPV$. (b) Schematic representation of the assembly of $(UPy)_2OPV$ and the reversible, UV-light and heat-induced dissociation.

The synthesis of the new $(UPy)_2OPV$ (**Figure 5b**) was possibly by coupling the known 1,4-bis(α-cyano-4-(12-hydroxydodecyloxy)styryl)-2,5-dimethoxybenzene with the known 2-(6-isocyanatohexylaminocarbonylamino)-6-methyl-4[1H]pyrimidinone. The as-prepared material showed the formation of a glassy material upon heating and cooling. A glass transition around 100°C was observed by DSC while fluorescence spectroscopy revealed a transition from orange-red excimer emission (626 nm) to green monomer emission (572 nm) upon heating $(UPy)_2OPV$ to above 125 °C (**Figure 6a**). This transition, which reveals the gradual dissociation of cyano-OPV motifs, was reversible upon slow cooling. Interestingly, the formation of monomer emission was also observed when a film of $(UPy)_2OPV$ was intentionally damaged with a razor blade (**Figure 6b**), demonstrating localized mechanically induced disassembly of cyano-OPV motifs. Upon irradiation with high intensity UV light (320-390 nm, 16s) the cut disappeared and upon rapid cooling a film displaying green fluorescence was obtained (**Figure 6c**). Equilibration of the sample at 120 °C (above T_g) resulted in the reappearance of excimer emission (**Figure 6d**). This behavior is consistent with thermally induced disassembly of both, the cyano-OPV and the UPy motifs after light-heat conversion upon irradiation with high intensity UV light; this liquefies the material so that the induced cut can heal rapidly and efficiently. Cooling presumably reassembles the UPy motifs and restores the glassy state. Depending on the cooling rate, the cyano-OPV motifs remain disassembled (**Figure 6c**) or re-assemble (**Figure 6d**). We are currently further investigating the exciting multi-stimuli-responsive nature of $(UPy)_2OPV$ in

more detail, focusing on the morphology and the binding states of the two motifs. We expect that the study can be completed with resources beyond this grant so that the work will become publishable.

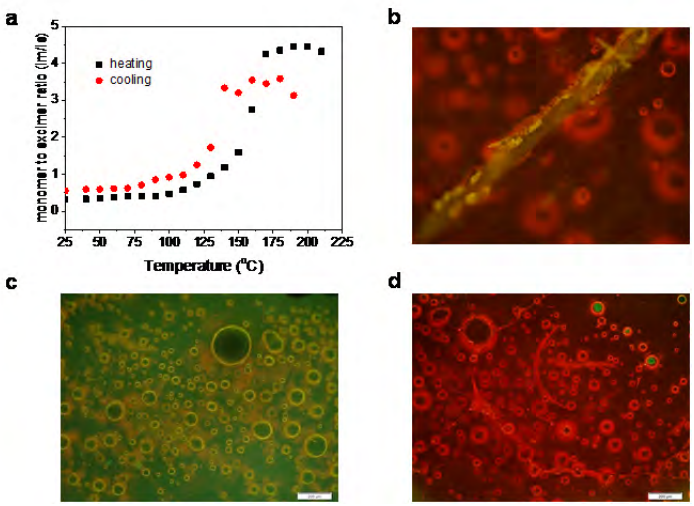

Figure 6. Properties of $(UPy)_2OPV$. (a) Monomer to excimer emission ratio of $(UPy)_2OPV$ as function of temperature. Fluorescence microscopy images of (b) a film of $(UPy)_2OPV$ that was cut with a razor blade; (c) the film shown in (b) after irradiation with UV light (320-390 nm, 16s); (d) the films shown in (c) after 90 min of equilibration at 120 °C. All optical microscopy images were recorded under illumination with 365 nm light.

Supramolecular Polymer Glasses

The results presented above, and also in previous reports in connection with this and previous ARO grants show nicely that the reversible and dynamic nature of non-covalent interactions between the constituting building blocks renders many supramolecular polymers stimuli-responsive. This feature has been exploited to create thermally and optically healable polymers, [4, 5, 6] but it proved challenging to develop materials that combine high stiffness and good healability.[7] In **Year 2**, we began the exploration of a glass-forming supramolecular polymer network based on a trifunctional low-molecular weight monomer ($(UPyU)_3TMP$) that carries ureido-4-pyrimidinone (UPy) groups (**Figure 7a**). In **Year 3**, we developed a new synthetic procedure that provides access to solvent-free $(UPyU)_3TMP$ (vide infra) and completed our study on the structure-property relationship of this material.

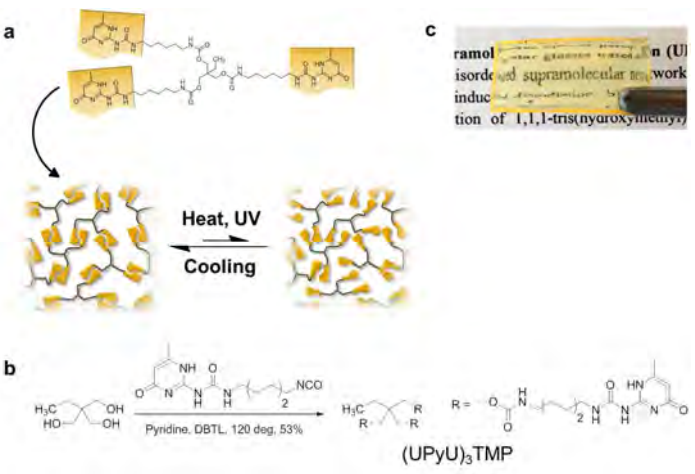

Figure 7. $(UPyU)_3TMP$ supramolecular polymer glass. (a) Schematic representation of the formation of a supramolecular networks based on $(UPyU)_3TMP$ and the reversible, heat- or light-induced dissociation. (b) Synthesis of $(UPyU)_3TMP$. (c) Image of a $(UPyU)_3TMP$ film.

Much of the previous work on UPy-based supramolecular polymers has focused on telechelic monomers with two terminal binding motifs that promote linear chain extension; this approach affords supramolecular polymers whose properties are to a large extent governed by the nature of the telechelic. By contrast, the trifunctional $(UPyU)_3TMP$ introduced here was designed to form supramolecular networks, whose properties are dictated by the cross-linked nature and the large weight-fraction of the binding motif. $(UPyU)_3TMP$ was prepared by reacting 1,1,1-tris(hydroxylmethyl)-propane with three equivalents of 2-(6-isocyanatohexylaminocarbonylamino)-6-methyl-4[1H]pyrimidinone using isocyanate chemistry (**Figure 7b**). In **Year 2** we used dimethyl-

formamide as solvent for this reaction, but discovered that the product thus obtained contained co-crystallized dimethylformamide, which proved difficult to remove and caused plasticization of the material. As a result, materials properties depended on the extent of residual solvent. In **Year 3**, we discovered that pyridine or dimethylsulfoxide both permit adequate solvation of the reactants and that precipitation with acetone afforded a solvent-free product; but reactions performed in pyridine yielded significantly less side products. Thus, we were able to conduct all material characterization experiments with $(UPyU)_3TMP$ that contained no residual solvent; while quantitatively somewhat different, all experiments confirmed the findings made with solvent-containing material.

The DSC first heating trace of the as-prepared $(UPyU)_3TMP$ shows a weak endothermic transition at 80 ºC, which is associated with the glass transition, and an endothermic peak at 178 ºC, corresponding to melting of the crystalline portion. The cooling scan reveals a glass transition around 100 ºC and is void of any other transitions, even at a cooling rate of 1 ºC min^{-1}, demonstrating that upon melting and cooling, $(UPyU)_3TMP$ forms an amorphous solid. This is confirmed by the second DSC heating trace, which also only shows a glass transition at 106 ºC. The interpretation of the DSC experiments was confirmed by powder X-ray diffraction experiments. The diffractogram of the as-prepared $(UPyU)_3TMP$ shows well-defined reflections, while the diffractogram of a sample that had been heated to 200 ºC and cooled to ambient only displays diffuse diffraction. Taken together, these data indicate that $(UPyU)_3TMP$ does not readily crystallize after being heated to form a melt; instead, the material forms a (kinetically trapped) amorphous glass, even when cooled very slowly.

$(UPyU)_3TMP$ can readily be melt-processed into solid supramolecular objects of various shapes by heating either the as-prepared crystalline monomer or material that had previously been converted into a glassy form to 200 ºC (i.e., above the T_m) to form of a clear, slightly viscous liquid. Subsequent cooling to room temperature, optionally in a mold, afforded a transparent hard material, for example in the form of self-standing films (**Figure 7c**) or coatings on substrates such as wood, glass, or paper (**Figure 8c**). Free-standing films were rather brittle and prevented characterization the mechanical properties by tensile testing or dynamic mechanical analysis. Therefore, a ca. 300 µm thin $(UPyU)_3TMP$ film was melt-deposited on a glass substrate, and the mechanical properties were investigated by depth-sensing indentation and atomic force microscopy (AFM) in force spectroscopy mode. The room-temperature Young's moduli – 3.7 ± 0.1 GPa determined by indentation (**Figure 8a**) and 2.7 ± 0.1 GPa measured by AFM (**Figure 8b**) – reflect a very high stiffness. Temperature-dependent AFM data reveal a significant modulus decrease upon heating, with an onset around 105 ºC (**Figure 8b**). A comparison with the DSC data makes evident that this stiffness decrease is associated with the transition from the glassy into a rubbery state. The AFM data permit the conclusion that the UPy-UPy interactions are not simply "switched off" when the $(UPyU)_3TMP$ supramolecular glass is heated above T_g; instead, a dynamic equilibrium between bound and dissociated states exists, which is shifted to the monomer side as the temperature is increased.

The high optical absorption imparted by the high UPy content, and the capability to dissociate into a low-viscosity melt should bestow the supramolecular $(UPyU)_3TMP$ glass with excellent optical healing capabilities. To test this, a piece of wood was coated with a 300 µm thin layer of amorphous $(UPyU)_3TMP$ and the coating was intentionally damaged by cutting with a razor blade. The damaged area was subsequently exposed to UV irradiation (320 – 390 nm, 500 $mW \cdot cm^{-2}$), which led to complete disappearance of the cut in as little as 12 s (**Figure 8c**). We employed AFM force spectroscopy measurements to determine the mechanical properties of the supramolecular $(UPyU)_3TMP$ glass in the pristine film, and after cutting and healing (**Figure 8d,e**). Gratifyingly, the load displacement curves, both loading and unloading, of the original and the healed material are identical, indicating quantitative restoration of the original mechanical properties (**Figure 8d**).

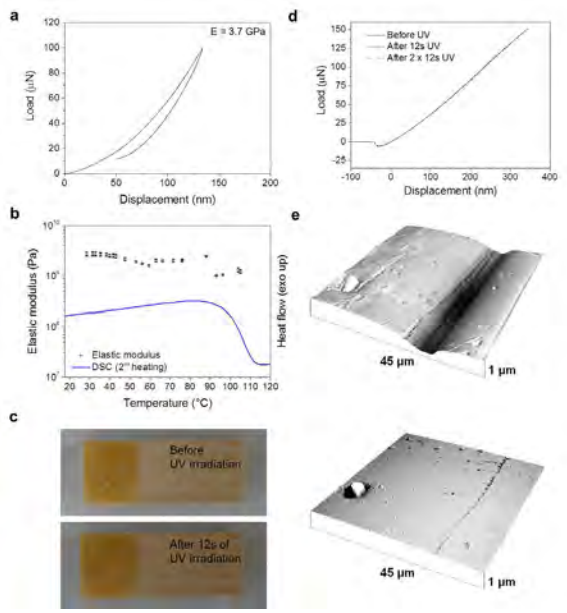

Figure 8. Properties of $(UPyU)_3TMP$ supramolecular polymer glass. (a) Load-displacement curve of a $(UPyU)_3TMP$ film acquired by depth sensing indentation. (b) Elastic moduli determined by AFM nanoindentation and heat flow determined by DSC as function of temperature. (c) Pictures showing the optical healing of a damaged $(UPyU)_3TMP$ coating on wood. The original coating was damaged (top) and subsequently exposed for 12 s to the light of a UV lamp, which caused complete healing (bottom). (d) Unloading curves of AFM nano indentation of an as-prepared (—) and a healed coating (—). (e) AFM images of damaged (top) and healed coating (bottom).

In **Year 3**, we also explored the possibility to use $(UPyU)_3TMP$ as debond-on-demand adhesive. Single lap joints were prepared by joining two glass substrates, of which one was coated with a 30 µm thin film of the glassy material, bonding them by heating to 200 °C for 10 sec, and cooling to ambient temperature. The lap joints displayed a shear stress of 1.2 ± 0.2 MPa, which is comparable to that of other supramolecular adhesives. When the bonded lap joints were placed under load and exposed to ultraviolet light (λ = 320-390 nm, 1000 $mW \cdot cm^{-2}$) the samples debonded within 30 sec. They could be re-bonded through exposure to light or heat, and the original adhesive properties were restored.

In summary, we have developed a novel optically responsive glass-forming supramolecular material which, in spite of the low-molecular weight nature of the building block, displays typical polymeric behavior, including high stiffness in the glassy state, viscoelastic behavior in the melt, and excellent coating and adhesive properties. Two specific characteristics appear to be particularly important in the context of the development of healable coatings. To our best knowledge the supramolecular $(UPyU)_3TMP$ glass is not only stiffer than any other optically healable polymer reported to date, but the material also heals much faster. This attractive combination of properties is a direct result of the design principle applied, i.e., the use of a low-molecular weight multifunctional building block to form a dynamic, disordered supramolecular network, which can readily be frozen into a glassy solid. This work has led to the submission of a US provisional patent application[8] that has been converted into a PCT application.[9] A manuscript detailing this work is currently under in-depth review at *Nature Chemistry*.[10]

Toughening of Supramolecular Polymer Glasses

Noting that $(UPyU)_3TMP$ is rather brittle, the remaining time of the PhD student working with this material was in **Year 3** focused on improving the toughness this material. Given that the structure of assembled $(UPyU)_3TMP$ is somewhat reminiscent of a highly cross-linked thermoset, our first attempt to reduce brittleness was the reduction of the crosslink density through the addition of a monofunctional UPy-containing chain stopper, which we surmised would decrease the cross-link density. To test this hypothesis, a mono-functional UPy-containing molecule was synthesized (UPy-C6-U-EH, **Figure 9c**) and melt-mixed in various ratios with $(UPyU)_3TMP$ to form a series of amorphous supramolecular glasses. DSC experiments show that the T_g of these glasses decreases with increasing content of UPy-C6-U-EH (**Figure 9a**). Rheological studies show that the addition of UPy-C6-U-EH also causes a shift of the storage and loss modulus traces to lower temperatures (**Figure 9b**). These results are characteristic of a reduction of the cross-link density and confirm clearly that the addition of the UPy-C6-U-EH chain stopper has the desired effect. Based on binding statistics one might expect that the addition of more than one equivalent of UPy-C6-U-EH would limit the formation of a supramolecular polymer network, the rheological behavior of mixtures comprising 1 and 1.5 equivalents of UPy-C6-U-EH are comparable, likely on account of phase separation at high concentrations of UPy-C6-U-EH.[10] While rubbery behaviour (associated with increased toughness compared to the glassy regime) was observed above T_g for $(UPyU)_3TMP$ and its blends with UPy-C6-U-EH, all materials remained brittle in the solid state.

Thus, we explored the introduction of a UPy-functionalized rubbery polymer to assure interaction with the supramolecular glass and therefore increase possible modes for stress relaxation. To this end we synthesized a UPy-functionalized PPO-PEG-PPO block copolymer (**Figure 9**) as toughener and also explored the use of PEG400 as commercially available plasticizer. Both additives feature PEG segments, which were chosen because the interaction of the ether linkages with the UPy motif is known to result in a shift of the UPy-UPy equilibrium to the monomeric form, hence a reduction of the crosslink density.[11] We surmised that this effect might promote the miscibility of the additives with $(UPyU)_3TMP$ in the melt, and would reduce the crosslinking density at the same time. Gratifyingly, preliminary results show that mixtures of $(UPyU)_3TMP$ with at least 10 wt% of added PEG400 or the UPy-functionalized PPO-PEG-PPO block copolymer are significantly toughened as indicated by ability to prepare thin self-standing films that allow us to perform DMTA and stress-strain experiments (ongoing). For mixtures of $(UPyU)_3TMP$ and PEG400 a drop in the glass transition and a shift of the rubbery regime to lower temperatures was observed (**Figure 9d**).

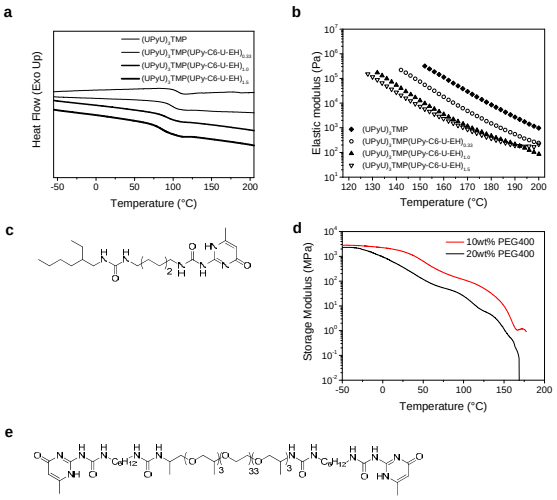

Figure 9. Toughening of $(UPyU)_3TMP$ supramolecular polymer glass. (a) Modulated differential scanning calorimetry (DSC) traces. (b) Elastic modulus (determined at $\gamma = 0.2\%$ and $\omega = 20$ rad·s^{-1}) as function of temperature. (c) Molecular structure of the chain stopper UPy-C6-U-EH. (d) Storage modulus as function of temperature. (e) Molecular structure of a UPy-functionalized PPO-PEG-PPO block copolymer

In summary, we have qualitatively demonstrated that it is possible to significantly toughen $(UPyU)_3TMP$, thereby creating glass-forming supramolecular materials which, in spite of the low-molecular weight nature of the building block, displays typical polymeric behavior. We believe that the work on toughened supramolecular glasses will be a significant step towards mechanically robust optically healable materials and possibly a new avenue to improve material properties of known molecular glasses.

Metallo-, Thermo- and Photo-Responsive Shape Memory and Actuating Liquid Crystalline Elastomers

Most of our previous ARO work has focused on healable and/or shape memory materials. To expand the repertoire of responses that we could access we focused in Year 3 on preparing multi-responsive liquid crystal elastomers, which will exhibit actuation in addition to soft shape memory characteristics.

It has recently been shown that liquid crystalline elastomers (LCE) are an interesting class of thermal shape memory polymers (SMPs).[12] In these materials, a nematic to isotropic liquid crystalline transition (rather than the more traditional T_g or T_m) provides the mobility transition within the polymer network required to deform the sample. Importantly, as cooling below this transition to fix the temporary shape does not result in a global vitrification of the sample, the material remains flexible in both its permanent and temporary shapes (unlike most thermal SMPs, which are generally stiff in their permanent shape) and as such can be considered "soft" SMPs.

Additionally, LCEs have garnered much interest as a consequence of their ability to act as stimuli-responsive actuators.[13, 14] When a stimulus induces a liquid crystalline to isotropic transition in a liquid crystalline material, the mesogenic units go from an oriented to non-oriented state. In an LCE these mesogens are tethered together in a polymeric network and the molecular motion of transition from an oriented to a non-oriented state is translated to macroscopic actuation.

We have previously developed Bip derivatives with an alkene containing alkyloxy substituent on the 5′ position (**1**) and have shown that they exhibit monotropic liquid crystalline behavior upon cooling from an isotropic melt.[15] Furthermore, this behavior is disrupted when exposed to various metal ions (e.g. $Zn(ClO_4)_2$, $Eu(NO_3)_3$, etc.), with these complexes exhibiting only isotropic

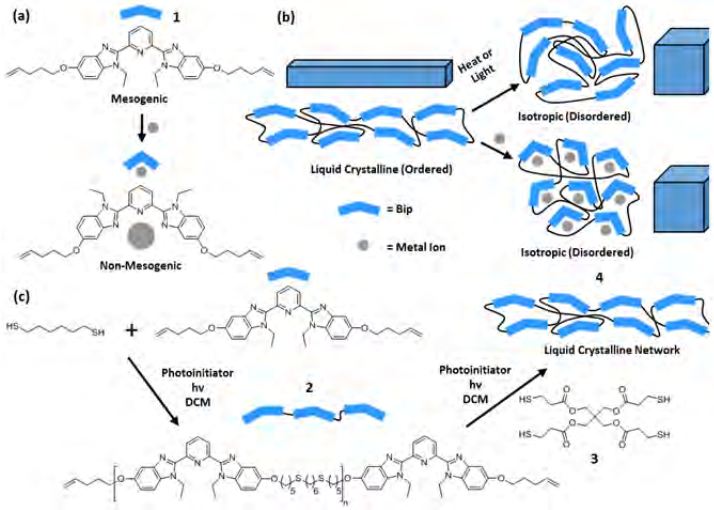

Figure 10. (a) Bip mesogens (**1**) display a conformational change upon binding a metal ion resulting in a change from mesogenic to non-mesogenic behavior. (b) Incorporation of Bip units into a liquid crystalline elastomer (LCE) network which is subsequently aligned by mechanical stretching results in a material which undergoes shape change in response to stimuli, such as heat, light or exposure to metal ions, which stimulate the liquid crystalline to isotropic transition. (c) Synthesis of Bip-containing LCEs via a two-step process wherein oligomers (**2**) are first produced via a photo-initiated thiol-ene reaction of **1** with 1,6-hexanedithiol. These oligomers are then cast in a Teflon mold and crosslinked using a second thiol-ene reaction of the oligomers with a tetrathiol crosslinking unit (**3**) thereby creating a Bip-LCE network (**4**).

behavior (**Figure 10a**). Acyclic Diene Metathesis (ADMET) polymerization of **1** allowed access to linear polymers that exhibit enantiotropic liquid crystalline behavior that could be "switched off" by the addition of a metal ion.[16] Building on this initial work, it was hypothesized that replacing conventional mesogens in a multidomain LCE with Bip-based mesogens (such as **1**) would result in a multi-responsive, soft shape-memory and actuating films where heat, light, or metal ions could be used to elicit the response (**Figure 10b**). In such systems, an alignment step would be needed prior to the actuation response in order to achieve the long range orientation order necessary for large contractile forces.

The targeted Bip-containing LCEs were prepared using a two-step thiol-ene approach (**Figure 10c**). A slight excess of the alkene Bip derivative **1**[15] was reacted with 1,6-hexanedithiol using a photo-initiated thiol-ene reaction, to access the Bip oligomers **2a-c** that had terminal alkene moieties. By controlling the ratio of **1**:hexanedithiol three different molecular weights of the oligomers **2** were obtained; molar ratios of **1**:hexanedithiol of 2:1, 6:5 and 9:8 yielded Bip oligomers of 1500 g/mol (**2a**), 4400 g/mol (**2b**) and 5800 g/mol (**2c**), respectively. The oligomers **2a-c** were then mixed with the tetrathiol crosslinker (**3**) (at a ratio of 1 thiol to 1 double bond) in dichloromethane, cast into a teflon mold and crosslinked using a second photo-initiated thiol-ene reaction.

All three films of **4** are opaque at room temperature and become transparent upon heating above 80°C (**Figure 11a**). DSC, XRD and POM (**Figure 11b**) experiments were performed on the films and confirm the presence of a liquid crystalline state with a LC-I transition at ca. 71-76 °C, depending on the sample **4a-c**. Stress-strain experiments were carried out to characterize the change in material properties upon heating above the liquid crystalline transition or exposure to metal ions. For example, at room temperature **4b** (**Figure 11c**) shows good elastomeric properties with ultimate elongation (ε_u) of 170% and ultimate tensile stress (σ_u) of 7.9 MPa. As expected for a LCE film heating them above their clearing point results in a significant increase in its elasticity and a drop in its strength. For example, at 100 °C **4b** has a ε_u of ca. 475% and σ_u of ca. 0.29 MPa.

One of the main goals of this study was to see if metal ions could be used to induce shape recovery and/or actuation of the film. Fe(II) ions were chosen as the metal ion since it is known that Bip complexes with Fe(II) are a deep purple color which allows easy visualization of the incorporation of the metal ion into the film.[17] The method chosen to introduce the Fe(II) into the film was to place it in a solution of the metal ion and allow the metal ion to diffuse into the film. With an eye toward metal ion induced switching studies it was important to find a solvent that allows the Fe(II) salt to diffuse into the film, but does not result in any solvent-

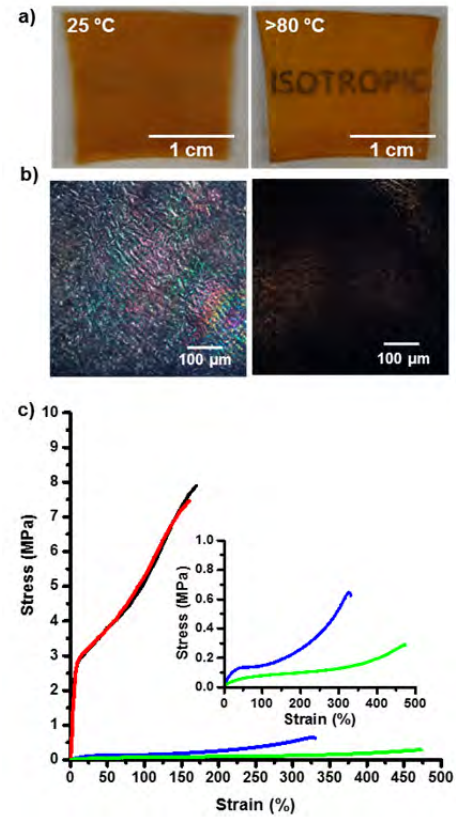

Figure 11. (a) Pictures of a film of **4b** at 25°C (left) and 80°C (right), (b) POM image of **4b** at r.t (left) and 100 °C (right). (c) Stress strain curves of **4b** in the neat state (—), in the neat state at 100 °C (—) after soaking for 20 min in 1mM $Fe(OTf)_2$ in 1:1 water:THF and subsequent drying (—), after soaking for 20 min in 1mM $Fe(OTf)_2$ in 1:1 water:THF followed by soaking for 1 hr in 10mM diethylene triamine in 1:1 water:THF and subsequent drying (—).

induced recovery of the material. A 1:1 mixture of water and THF was determined to be a good "middle ground" solvent system, which did not induce any significant swelling in the film but provided an appropriate environment to infuse the samples with metal ions. Thus submersion of a film of **4b** in 1 mM $Fe(OTf)_2$ dissolved in 1:1 water:THF results in a dramatic change in color of the film (yellow-purple) consistent with the incorporation of Fe^{2+} into **4b**. Upon drying the Fe(II)-imbibed film **4b·Fe(OTf)$_2$** is much more elastic and softer than Fe(II)-free films (ε_u of 330% and σ_u of 0.64 MPa), as can been by the stress-strain curves in **Figure 11c**. In fact these properties more closely resemble the properties of **4b** when isotropic (i.e. at higher temperatures). Furthermore, the **4b·Fe(OTf)$_2$** films exhibit no birefringence under POM nor exotherm upon cooling and show only a broad diffuse scattering at 4.16 Å in XRD. As such, these data are consistent with metal ion binding "turning off" the liquid crystallinity of the LCE and converting the film at room temperature to an isotropic state. If this is the case then removing the Fe(II) from the film should result in recovery of the properties of the material. Gratifyingly, when a film of **4b·Fe(OTf)$_2$** is exposed to a solution of 10 mM diethylene triamine the deep purple color of the film is removed and both the birefringent pattern the mechanical properties (**Figure 11c**) of the de-metallated film are restored to close to those of the original film.

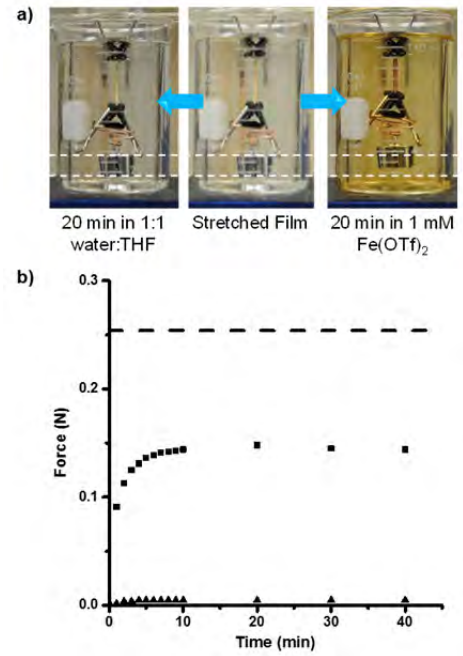

Figure 11. (a) A film of **4b** that had been previously heated, stretched to 100% strain and then cooled in the stretched state holds a 10 g mass in a beaker of 1:1 water:THF. After 20 min no actuation is observed. $Fe(OTf)_2$ is added and stirred to produce a 1 mM solution. (b) Actuation force generated by a 0.3 mm x 4 mm x 10 mm vs immersion time in a 1 mM $Fe(OTf)_2$ solution in 1:1 water:THF (■) and 1:1 water:THF with no metal ion (▲). The dashed line represents the maximum force achieved for the same sample when irradiated with UV light with an intensity of approximately 500 mW/cm^2 in the wavelength range of 320 – 390 nm with a peak at 365 nm. In all instances the sample had previously been heated above the LC transition, strained to 100% strain, and then cooled to room

The shape-memory properties of the LCE **4b** were then evaluated using dynamic mechanical thermal analysis (DMTA). Heating the films to 100 °C, straining them to 75% and then cooling them before releasing the strain showed the films exhibited a degree of fixing of ca. 99% (as defined by ε_u / ε_u where ε_m is the maximum strain and ε_u is the strain after unloading). Reheating the stretched fixed film to 100 °C results in the films recovering to ca. 98% of its original length. A similar degree of fixing and recovery is observed over at least 5 cycles.

Having shown shape memory properties the next goal was to see if these films act as an actuator. In these experiments a film of **4b** that had previously been heated above the liquid crystalline clearing temperature, stretched to 100% strain and cooled, was attached to a 10 g weight (**Figure 12a**). The sample was then suspended in a beaker of 1:1 water:THF (**Figure 12a** middle). After 20 minutes no actuation was observed (**Figure 12a** left). $Fe(OTf)_2$ was then added to the solution along with brief stirring to produce a 1 mM solution. After 20 minutes the film had noticeably lifted the mass (**Figure 12a** right). This demonstrated that simple plasticization of the sample with the solvent was

insufficient to achieve appreciably actuation of the sample but the binding of the metal ion to the Bip can indeed generate enough force to lift a 10 g weight.

To further quantify the actuation force generated by this material, a film with dimensions of 0.3 mm x 4 mm x 10 mm was heated above the LC transition, stretched to 100% strain and then cooled to room temperature. The sample was then clamped in a tensile tester under zero load and zero strain rate. The sample was irradiated with UV light with an intensity of approximately 500 mW/cm^2 in the wavelength range of 320 – 390 nm and a λ_{max} of 365 nm. The Bip ligand is known to absorb UV light in this range with significant conversion to heat resulting in a dramatic increase in sample temperature. As the sample absorbs light it is heated above the LC transition which in turn triggers the contraction. The resulting contraction force is measured by the load cell on the tensile tester under the isostrain conditions and showed that the maximum force achieved by the sample under these conditions was 0.254 N (212 kPa) (**Figure 12b** dashed line) which is typical for an LCE actuator.

The actuation force upon exposure the metal ion salt solution (1 mM in 1:1 water:THF) was then examined. A sample with dimensions 0.3 mm x 4 mm x 10 mm was heated above the LC transition, stretched to 100% strain and cooled to room temperature. The sample was then clamped in a tensile tester under zero load and zero strain rate. A submersion chamber was fitted to the apparatus and was filled with a 1 mM $Fe(OTf)_2$ solution in 1:1 water:THF. The resulting actuation force was measured by the load cell in the isostrain state and readings were taken every minute for the first ten minutes and then every ten minutes until the force equilibrated. The maximum force achieved using this method was 0.148 N (**Figure 12b** squares). As a control, this experiment was repeated using a 1:1 water:THF solution with no metal ions. Under these conditions no significant actuation force was observed (**Figure 12b** triangles).

In summary, with the goal of preparing multi-responsive polymer actuators, we have incorporated liquid crystalline metal-binding Bip monomers into polymeric networks via thiol-ene chemistry. These crosslinked films exhibit liquid crystalline behavior which can be harnessed to access soft shape memory with excellent thermal fixity and recovery. The permanent shape of these multi-domain LCEs can also be recovered via exposure to metal ions at room temperature, presumably as the metal ion binding results in a liquid crystal to isotropic transition. This process is reversible, as the removal of metal ions from the film with diethylene triamine yields a return towards the original properties of the material. Furthermore, we have shown that long range alignment of the mesogens can be achieved through physical stretching above the LC transition temperature. The conversion from the stretched aligned to contracted isotropic state can be achieved via a thermo-, photo- or metallo- stimulus resulting in a contractile force in the material which can be as high as 0.254 N. This work was published in *Macromolecules* this year.[18]

References

[1] Coulibaly, S.; Heinzmann, C.; Beyer, F.L.; Balog, S.; Weder, C.; Fiore, G.L.; Supramolecular Polymers with Orthogonal Functionality; *Macromolecules* **2014**, *47*, 8487−8496.

[2] Kumpfer, J.R.; Wie, J.J.; Swanson, J.P.; Beyer, F.L.; Mackay, M.E.; Rowan, S.J.; Influence of Metal ion and Polymer Core on the Melt Rheology of Metallo-Supramolecular Films; *Macromolecules*, **2012**, *45*, 473-480.

[3] Makowski, B.; Kunzelman, J.; Weder, C.; Stimuli-Driven Assembly of Chromogenic Dye Molecules: A Versatile Approach for the Design of Responsive Polymers; In: *Handbook of Stimuli-Responsive materials*; Urban, M., Ed.; Wiley-VCH, New York, **2011**, 117-138.

[4] Burnworth, M.; Tang, L.; Kumpfer, J.R.; Duncan, A.J.; Beyer, F.L.; Fiore, G.L.; Rowan, S.J.; Weder, C.; Optically Healable Supramolecular Polymers; *Nature* **2011**, *472*, 334-337.

[5] Biyani, M.V.; Foster, E.J.; Weder, C.; Light-Healable Supramolecular Nanocomposites Based on Modified Cellulose Nanocrystals; *ACS Macro Letters* **2013**, *2*, 236−240.

[6] Coulibaly, S.; Roulin, A.; Balog, S.; Biyani, M.; Foster, E.J.; Rowan, S.J.; Fiore, G.L.; Weder, C.; Reinforcement of optically healable supramolecular polymers with cellulose nanocrystals; *Macromolecules* **2014**, *47*, 152-160.

[7] Fiore, G.; Rowan, S.J.; Weder, C.; Optically Healable Polymers; *Chem. Soc. Rev.* **2013**, *42*, 7278-7288.

[8] Weder, C.; Balkenende, D.; Fiore, G.L.; Stimulus-Responsive Supramolecular Glasses; US Provisional Patent Application 61/939,893 filed 2014.

[9] Weder, C.; Balkenende, D.; Fiore, G.L.; Stimulus-Responsive Supramolecular Glasses; PCT filed 2015.

[10] Balkenende, D.W.R.; Monnier, C.A.; Fiore, G.L.; Weder, C.; Optically responsive supramolecular polymer glasses; *Nature Chemistry* **2015**, *Submitted*

[11] de Greef, T. F. A.; Nieuwenhuizen, M. M. L.; Sijbesma, R. P.; Meijer, E. W., Sijbesma, R. P.; Meijer, E. W. Competitive Intramolecular Hydrogen Bonding in Oligo(ethylene oxide) Substituted Quadruple Hydrogen Bonded Systems. *J. Org. Chem.* **2010,** *75*, 598-610.

[12] Burke, K.A.; Mather, P.T. *J. Mater. Chem.* **2010**, *20*, 3449-3457.

[13] Jiang, H.; Li, C.; Huang, X. *Nanoscale* **2013**, *5*, 5225-5240.

[14] Ohm, C.; Brehmer, M.; Zentel, R. *Adv. Mater.* **2010**, *22*, 3366-3387.

[15] McKenzie, B.M.; Miller, A.K.; Wojtecki, R.J.; Johnson, J.C.; Burke, K.A.; Tzeng, K.A.; Mather, P.T.; Rowan, S.J. *Tetrahedron* **2008**, *64*, 8488-8495.

[16] McKenzie, B.M.; Wojtecki, R.J.; Burke, K.A.; Zhang, C.; Jakli, A.; Mather, P.T.; Rowan, S.J. *Chem. Mater.* **2011,** *23*, 3525-3533.

[17] Krumholz, P.; Orquima, S. A. *Inorg. Chem.* **1965**, *4*, 612-616.

[18] Michal, B.T.; McKenzie, B.M.; Felder S.E.; Rowan S.J.; Photo-, Thermo- and Metallo-Responsive Shape Memory and Actuating Liquid Crystalline Elastomers; *Macromolecules*, **2015**, *48*, 3239-3246.